ELSEVIER

Journal of Power Sources 83 (1999) 1–8

JOURNAL OF POWER SOURCES

www.elsevier.com/locate/jpowsour

Thermal modeling and design considerations of lithium-ion batteries

S. Al Hallaj, H. Maleki, J.S. Hong, J.R. Selman *

Center for Electrochemical Science and Engineering, Department of Chemical and Environmental Engineering, Illinois Institute of Technology, Chicago, IL 60616, USA

Received 15 September 1998; received in revised form 4 January 1999; accepted 25 January 1999

Abstract

A simplified one-dimensional thermal mathematical model with lumped parameters was used to simulate temperature profiles inside lithium-ion cells. The model makes use of heat-generation parameters established experimentally for the Sony (US18650) cell. The simulation results showed good agreement with temperature measurements at $C/2$, $C/3$, and $C/6$ discharge rates, while some deviation was noticed for the $C/1$ discharge rate. The model was used to simulate temperature profiles under different operating conditions and cooling rates for scaled-up cylindrical lithium-ion cells of 10 and 100 A h capacity. Results showed a strong effect of the cooling rate on cell temperature for all discharge rates. A significant temperature gradient inside the cell was found only at higher cooling rates, where the Biot number is expected to be > 0.1. At lower cooling rates, the cell behaves as a lumped system with uniform temperature. To establish the limits of temperature allowable in scale-up by the simplified model, commercial lithium-ion cells at different open circuit potentials were tested inside an accelerated rate calorimeter (ARC) to determine the onset-of-thermal-runaway (OTR) temperatures. Sony (US18650) cells at 4.06, 3.0, and 2.8 V open circuit voltage (OCV) were tested and their measured OTR temperatures were found to be 104, 109, and 144°C, respectively. A sharp drop in the OCV, indicating internal short circuit, was noticed at temperatures close to the melting point of the separator material for all open circuit voltages.

Keywords: Thermal modeling; Thermal runaway; Sony cell; Li-ion cells; Scale-up design

1. Introduction

Lithium-ion 'rocking-chair' batteries in small sizes (e.g., AA-size) are widely used to power personal electronic devices because of their high voltage (> 4.0 V) and high energy density (~ 265 (W h) L^{-1}). Lithium-ion batteries potentially have 4–5 times higher power density than lead-acid batteries, but thermal stability problems must be overcome. These batteries are investigated as a potential power source for electric vehicles (EV) to provide longer driving range, adequate acceleration, and long lifetime.

The primary challenge in designing a scaled-up lithium battery system (1–4 kW h) is safety, under abusive as well as normal operating conditions. During battery charge/discharge, various chemical and electrochemical reaction as well as transport processes take place. Some of these reactions and processes continue also under open circuit conditions. They are largely exothermic and may cause heat to accumulate inside the battery if heat transfer from the battery to the surroundings is not sufficient. This may be the case if the battery is operated under insulating conditions or in a hot environment. It will cause battery temperature to rise significantly, so 'hot spots' may form within the battery, thereby risking thermal runaway.

Performance and thermal modeling in combination are essential tools in optimizing the design of scaled-up cells and batteries for automotive applications. Models of this type are capable of accounting for battery performance and durability. However, they may require as input many system properties, as well as operational parameters. Of these properties, for example, transport properties, thermodynamic properties and heat effects, are difficult to estimate quantitatively. Extensive experimental measurements may be required to evaluate these quantities and to develop a clear understanding of the role of different cell components (electrodes, electrolyte and separator) in heat generation as well as cell performance. However, for the purpose

* Corresponding author: Tel.: +1-312-567-3970; Fax: +1-312-567-6914; E-mail: selman@charlie.cns.iit.edu

0378-7753/99/$ - see front matter
PII: S0378-7753(99)00178-0

of cell design a relatively simple model based on a limited number of measurements may have much merit. The main objective of this paper is to present such a relatively simple model and explore its limitations.

In earlier work the heat effect of a commercial cell (Sony US18650) was measured using an Accelerated Rate Calorimeter (ARC) in combination with a battery cycler, during cycling over a range of operating parameters within the limits recommended by the manufacturer [1,4]. An integral energy balance applied to the cell was used to determine the total heat generated by the cell during cycling.

Calorimetric techniques in combination with electrochemical measurements may also be applied to cell components such as electrodes and separators. Integrated implementation may then provide valuable information about cell and component properties, behaviour, and characteristics. However, as will be shown, detailed knowledge of component behaviour is not necessary for a first approach to optimized scale-up, for example, using simplified transient one-dimensional thermal model with lumped parameters. It is the objective of this work to demonstrate the validity of such an approach to simulate the thermal behaviour of scaled-up Li-ion cells.

In this work we further present some thermal runaway data for the Sony (US18650) cell at different open circuit voltages. These data allow us to indicate, in a preliminary fashion, expected limits on the scale-up of batteries that have a similar chemistry as the Sony battery.

2. Temperature effect on cell and battery performance

Temperature excursions and non-uniformity of the temperature are the main concern and drawback for any attempt to scale-up lithium-ion cells to the larger sizes desirable for high power applications as in EV propulsion systems. Basically, battery design requires a trade-off between the risk of overheating individual cells of relatively large sizes, and the cost of insulating or cooling a complex array of small cells. However, this trade-off can be assumed to yield an optimum cell size that is significantly larger than the presently commercial Li-ion cells (somewhat larger than AA-size). Thus, a well-designed thermal management system is required to ensure good battery performance, safety, and higher capacity. Thermal management systems using active cooling (forced circulation of air or liquid) have been proposed and simulated for lead-acid batteries in electric vehicle applications [5]. Simulation results showed that thermal management systems of this kind might improve battery performance by 30–40%. However, such active cooling systems introduce another level of complexity in the design and operation of the battery system.

The thermodynamics of lithium-ion cells are complicated by the presence of liquid electrolyte mixtures as well as single-phase and multiphase solids. Heat generation may result from mixing and phase change, as well as the main electrochemical reactions. Reliable prediction of temperature profiles of individual cells, and of a battery system as a whole requires first of all quantitative evaluation of the total heat generation rate. Thus, measurements of temperature rise and heat dissipation of small cells, are essential for simple but accurate modeling of scaled-up batteries. It would be advantageous to keep such a model relatively simple, by focusing on the cell as a whole, its geometry and its total heat generation rates.

3. Thermal modeling of Li batteries

Thermal models for batteries simulate temperature profiles inside the battery/cell during charge and discharge. Models available in the literature vary from relatively simple one-dimensional thermal models [6–14], assuming simplified cell design and mode of operation (isothermal, constant current, lumped thermophysical properties, and constant heat generation rates), to comprehensive three-dimensional models with non-isothermal, temperature-dependent thermophysical properties and heat generation rates [15,16]. These models describe in detail the heat effects caused by ohmic resistance, chemical reactions, mixing processes, polarization and electrode kinetic resistance. Such models also presuppose a thorough understanding of the thermodynamic properties of battery materials and parts.

However, as shown in Ref. [14], for cell performance model under normal conditions of battery use, lumped properties and heat generation rates are sufficient. For such an application, a minimum set of data is necessary to develop a satisfactory model to predict the thermal behaviour of Li-ion batteries. In the following, we present a one-dimensional mathematical model to simulate the temperature profile of cylindrical cells. The heat generation rates required as input in the computer simulation are estimated from experimental measurements of overpotential and entropy of reaction (reversible heat effect) during a cycle.

4. Model development and theory

An unsteady-state one-dimensional (radial direction) thermal mathematical model was developed to simulate the temperature profile in the battery during discharge. It treats the cell as a thermally homogenous body with effective thermophysical properties. The cell properties are assumed to be independent of temperature over the range of operation temperatures. Heat is assumed to be generated uniformly throughout the cell.

The energy balance in the cell is described by Eq. (1) and the boundary conditions are described in Eqs. (2) and

(3). The cell temperature is initially uniform and equal to the ambient temperature, as shown in Eq. (4).

$$\frac{\partial^2 T}{\partial r^2} + \frac{1}{r}\frac{\partial T}{\partial r} + \frac{q}{k_{\text{cell}}} = \frac{1}{\alpha}\frac{\partial T}{\partial t} \quad (1)$$

$$\left.\frac{\mathrm{d}T}{\mathrm{d}r}\right]_{r=0} = 0 \quad (2)$$

$$-k_{\text{cell}}\left.\frac{\mathrm{d}T}{\mathrm{d}r}\right]_{r=R} = h(T - T_{\text{a}}) \quad (3)$$

$$T = T_{\text{a}} \text{ at } t = t_{\text{o}} \text{ and for all } r. \quad (4)$$

The volumetric heat generation rate, q, includes heat generation by overvoltage and chemical reactions, and neglects any other heat effect (e.g., heat of mixing). Part of the heat generated remains inside the battery as sensible heat. Another part of the heat generated inside the cell during discharge is conducted through the cell layers and then transferred to the surroundings through the cell surface. Evans and White [29] reported that the heat transfer resistance of spirally wound $Li/SOCl_2$ cell in the radial direction was twenty times higher than that in the axial direction. Similar results were found and reported by our group for the Sony US 18650 cell, as reported elsewhere [17]. Therefore, the present model is restricted to the radial heat transfer only.

5. Heat generation rates

Heat generation rate inside the cell is derived from the governing thermodynamic relations described in Eqs. (5)–(9):

$$Q = \Delta G + T\Delta S + W_{\text{el}} \quad (5)$$

$$\Delta G = -nFE_{\text{eq}} \quad (6)$$

$$\Delta S = nF\frac{\mathrm{d}E_{\text{eq}}}{\mathrm{d}T} \quad (7)$$

$$W_{\text{el}} = -nFE \quad (8)$$

$$Q' = I\left[\left(E_{\text{eq}} - E\right) + T\frac{\mathrm{d}E_{\text{eq}}}{\mathrm{d}T}\right] \quad (9)$$

Eq. (9) is similar to the general energy balance presented earlier by Gibard [23] and is the summation of the reversible and the irreversible heat effects. In this work the overpotential was measured experimentally, while the entropy term was estimated from the entropy coefficient $(\mathrm{d}E_{\text{eq}}/\mathrm{d}T)$ measured experimentally as described earlier [1].

6. Results and discussions

6.1. Normal conditions—experimental data

The cell voltage on load of the Sony US 18650 cell was measured experimentally at different depths of discharge (DOD) for $C/1$, $C/2$, $C/3$, and $C/6$ discharge rates at 35°C operating temperature, specifications and chemistries of the cell are listed in Table 1. The open circuit voltage is assumed to be equal to the equilibrium potential and was measured experimentally by DC-current interruption at different depths of discharge. This was achieved by discharging the cell at $C/6$ discharge rate, then interrupting the current for 3 h while cell voltage and temperature are monitored during that period. The cell temperature at the end of interruption always had returned to its initial value; this was important to eliminate any temperature effect on the measured open circuit voltage (OCV) values. In any case, the temperature rise at the end of discharge for normal $C/6$ discharge rate under ARC operating conditions without interruption was less than 4°C, which is further assurance of negligible deviation of OCV due to heat retained in the cell.

Fig. 1 shows the measured OCV and cell voltage on load for all discharge rates at different depths of discharge. The measured OCV values between 0.5–0.75 depths of discharge were found to be less than the cell voltage on load at $C/6$ discharge rate. This may be explained by the relatively short relaxation time (3 h) used in this experiment, since it is known that complete relaxation in this range may take days or even weeks [2]. It could also be related to the reported hysteresis of Li-ion batteries in this region [3]. For all discharge rates, the difference between OCV and cell voltage on load, at different depths of discharge, was considered to be the overvoltage. These values were used in Eq. (9) to calculate the irreversible heat effects.

For the entropy coefficient $(\mathrm{d}E/\mathrm{d}T)$ of Sony cells, values of -0.429 and -0.753 mV K^{-1}, at OCV = 4.044 and 3.227 V, respectively, were measured and reported earlier by our group [1]. In this work linearly interpolated values were used at other depths of discharge, to calculate the reversible (entropic) heat effects. Results for reversible and irreversible heat effects are shown in Fig. 2. At lower discharge rates ($C/2$, $C/3$ and $C/6$), most of the heat generated during cell discharge is reversible (entropic). This is in agreement with the results of our earlier work [1], which showed that 40–60% of the heat generated at $C/1$, $C/2$ and $C/3$ discharge rates is due to entropic effects. Total heat generation rates for this work at $2C$,

Table 1
Specification for the Sony (US18650) cell

Capacity: 1.35 A h
Diameter, $D = 18$ mm; height, $L = 65$ mm
Height-to-diameter ratio, $L/D = 3.61$
$k_{\text{eff}} = 3.0$ W (m °C)$^{-1}$; $C_p = 1.0$ J (g °C)$^{-1}$
Cut off voltages = 2.5 and 4.2 V for discharge and charge, respectively
Cathode material: $LiCoO_2$
Anode material: disordered carbon
Electrolyte: PC + DEC/$LiPF_6$
Separator: polypropylene and polyethylene

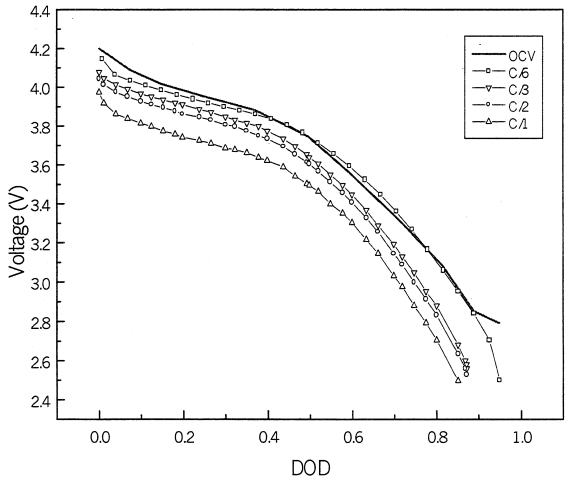

Fig. 1. Open circuit voltage and cell voltage on load vs. DOD (Sony Type US18650), at $C/1$, $C/2$, $C/3$, and $C/6$ discharge rates.

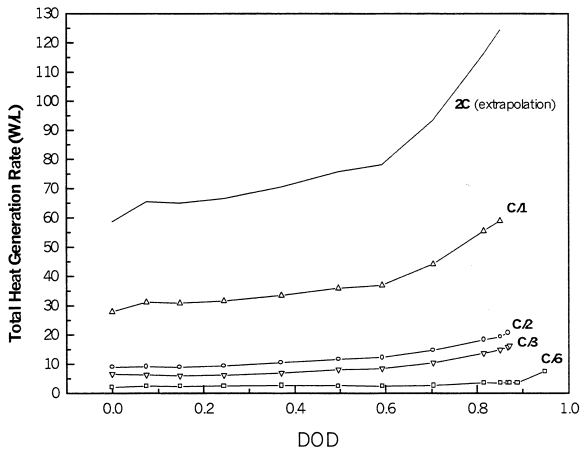

Fig. 3. Volumetric heat generation rate for the Sony US18650 cell at $2C$, $C/1$, $C/2$, $C/3$, and $C/6$ discharge rates.

$C/1$, $C/2$, $C/3$ and $C/6$ are shown in Fig. 3. The calculated values of the heat generation rate were linearly extrapolated at different DODs to estimate the heat generation rate at $2C$ discharge rate. Heat generation rates increase sharply at the end of discharge. This is consistent with the sharp increase of the measured overvoltage (impedance) of the cell at the end of discharge, due to the high concentration polarization.

6.2. Normal conditions—temperature profile

Eq. (1) was used to simulate the temperature profile inside the cell. Thermal properties needed for the computer simulation, listed in Table 1, were taken from measurements reported elsewhere [17]. Simulation results for the Sony cell, at all discharge rates, are shown in Fig. 4. These are in good agreement with experimental measurements for $C/2$, $C/3$ and $C/6$ discharge rates, while some deviation is noticed for $C/1$ discharge rate. This may be due to the assumption that heat is generated uniformly throughout the cell, which may not be true if discharge takes place rapidly. At high discharge rates the temperature build-up near the center may accelerate the local reaction rate and cause an earlier onset of the irreversible heat generation. At slower discharge rates, irreversible heat generation dominates only near the end of discharge. Alternatively, the rapid discharge rate may not leave enough time for endothermic transformations to go to completion. At low discharge rates uniformity is more likely, hence, simulated results match the measured values.

At the $2C$ discharge rate, the cell temperature is expected to rise significantly toward the end of discharge. If the initial temperature of the cell was higher than the one shown in this work or if the cooling rate is lower ($h < 10$

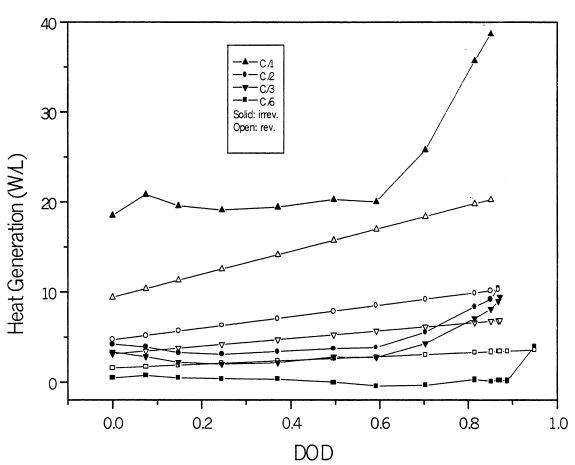

Fig. 2. Reversible and irreversible heat effects vs. DOD, for Sony Type (US18650) cell at $C/1$, $C/2$, $C/3$, and $C/6$ discharge rates.

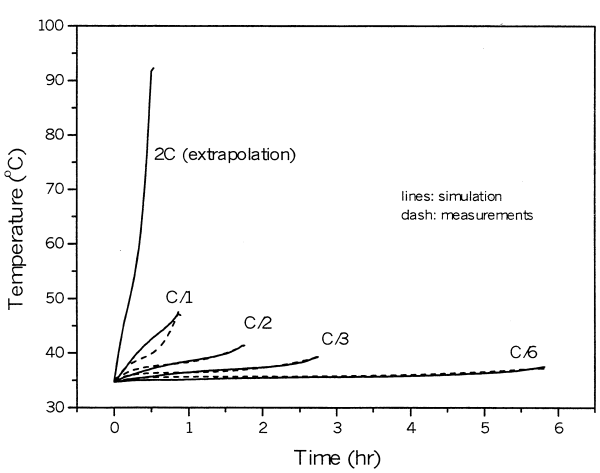

Fig. 4. Simulation results against temperature measurements for Sony Type US18650 cell at all discharge rates. $T_a = 35$°C, and $h = 10$ W m^{-2} K^{-1}.

W m^{-2} K^{-1}), the cell temperature may be expected to reach onset-of-thermal-runaway (OTR) temperature.

Johnson and White [25] showed that the Sony cell can operate at 2*C* and 3*C* rates without risking thermal runaway. However, the utilized portion of the nominal capacity of the cell at 2*C* and 3*C* discharge rates were about 50 and 15%, respectively. This is due to the use of coke-based anode in the Sony cell which sacrifice energy density for excellent cycle life and performance. As a result, the temperature rise of the cell did not reach OTR temperature, since only small part of the cell was utilized at these high discharge rates. While in the simulation part for the 2*C* rate for the Sony cell in this work, we assumed that 80% of the nominal capacity is utilized which allowed the temperature of the cell to reach the OTR temperature.

6.2.1. Thermal runaway conditions

To establish the limits of application of the model, thermal runaway tests were carried out. The results were compared with temperature profile predictions for the critical temperatures observed. Fig. 5 illustrates thermal runaway tests for Sony cells at different depths of discharge. All experiments were conducted inside an Accelerated Rate Calorimeter (ARC 2000, Columbia Scientific) in combination with a battery cycler (Model BT 2042, Arbin Instruments). In each experiment, the cell was placed inside the ARC and heated stepwise to thermal runaway conditions. The cell temperature was measured using an E-type thermocouple attached to the cell surface. The experimental sequence is based on the ARC heat–wait–search (HWS) mode, where the cell temperature is increased 5°C in each step followed by 15 min wait time. During wait time, the self-heating rate (SHR) of the cell is monitored carefully. If the detected SHR is larger than 0.2°C min^{-1}, this is considered an indication of the onset of an exothermic reaction. The ARC then shuts down the heating and records cell temperature till the end of the thermal runaway process. Details about the ARC operating modes and specifications can be found elsewhere [18,19].

The OTR temperatures at 4.06, 3.0 and 2.8 V open circuit voltages, were found to be 104, 109, and 144°C, respectively, as shown in Fig. 1a–d. The measured open circuit voltage drops sharply during the thermal runaway reaction and indicates an internal short circuit of the cell at temperatures between 145–150°C for all open circuit voltages. This is close to the melting point of polyethylene-based material used as a separator in the Sony cells [22,25]. These experiments demonstrate that the OTR temperature for Li-ion cells drops significantly, from 145 to 109°C, if the cell is only slightly charged. Saito et al. [2], studied the current and temperature behaviour of Sony cells at different states of charge (SOC) under short circuit conditions. Initial peaks of current and temperature after short circuit were noticed, followed by a breakdown of the

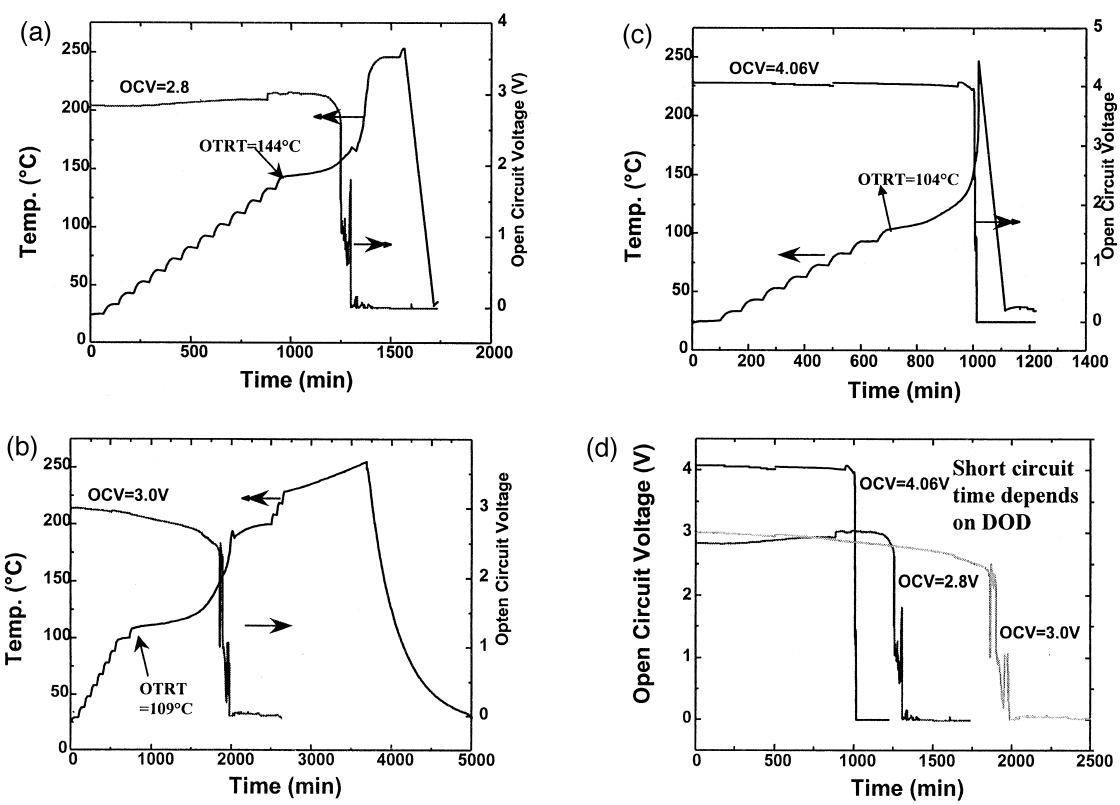

Fig. 5. Thermal runaway experiments for Sony (US18650) Li-ion cell. (1a) OCV = 2.8 V, (1b) OCV = 3.0 V, (1c) OCV = 4.0 V, and (1d) OCV vs. time.

Table 2
Dimensions for scaled-up cells

Capacity (A h)	$L/D=3$		$L/D=4$	
	D (mm)	L (mm)	D (mm)	L (mm)
10	37.4	112.3	34.0	136.0
100	80	240	73.3	293.0

cell separator at temperatures above 120°C. However, the cells at low SOC took more time to reach the shutdown or breakdown temperature. Therefore, regardless of other conditions for cell storage, it is recommended to store these cells in the fully discharged states. In the scale-up design calculation we adopted the following as local temperature limits.

6.2.2. Scaled-up design

Sony, SAFT, and other battery companies have recently designed and tested scaled-up Li-ion cells for EV application [26–28]. However, little or no data concerning their performance and thermal behaviour are available in the literature. Maeda et al. [20] reported a 25°C temperature increase at the end of $C/1$ discharge rate for a graphite–coke/$LiCo_{0.3}Ni_{0.7}O_2$ 30 A h cell. The cell has a cylindrical design with 60 and 185 mm diameter and height, respectively ($L/D \sim 3$). Kanari et al. [21,24] carried out thermal simulation for an 10–100 A h scaled-up carbon/Li_xCoO_2 cells, to study the effect of cell design and operating conditions on the temperature change of the cell. The cells were assumed to have an $L/D \sim 3$ aspect design ratio. Simulation results showed a temperature increase of 4 and 8°C for the 1 and 30 A h cells, respectively, at the end of a $0.2C$ discharge with $h = 10$ W m^{-2} K^{-1}. In both cases the temperature difference between the cell surface and center was less than 2°C. For a 10 A h scaled-up cell at 0.2C discharge rate, a temperature rise of 4 and 20°C for $h = 100$ and 1 W m^{-2} K^{-1}, respectively, were estimated.

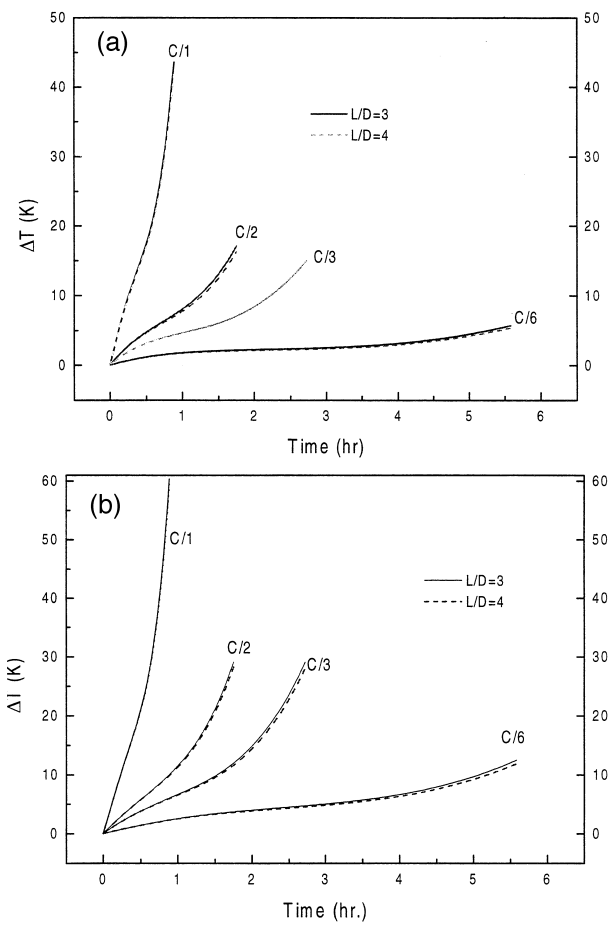

Fig. 6. (a) Simulated temperature profile for the 10 A h cell at all discharge rates, $h = 10$ W.m^{-2}.K^{-1}. (b) Simulated temperature profile for the 100 A h cell at all discharge rates, $h = 10$ W m^{-2} K^{-1}. ΔT: Transient temperature increase at the center of the cell. L/D: Cell-length-to-height ratio.

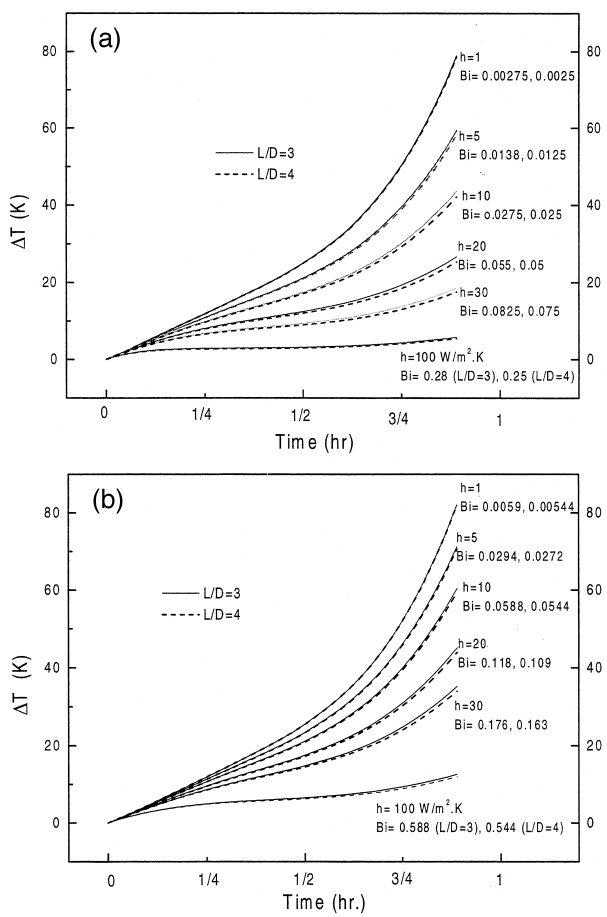

Fig. 7. (a) Simulated temperature profile for the 10 A h cell under different cooling conditions, discharge rate = $C/1$. (b) Simulated temperature profile for the 100 A h cell under different cooling conditions, discharge rate = $C/1$. ΔT: Transient temperature increase at the center of the cell. L/D: Cell-length-to-height ratio.

Utilizing information and measurements available for the Sony cell, we projected design for scaled-up cylindrical Li-ion cells, of 10 and 100 A h capacity, respectively. The cells are assumed to be assembled from materials similar to those used in the Sony cell so that the thermal properties are the same. The sizes of the scaled-up cells were determined based on the nominal energy density for the Sony cell, i.e., 80 (A h) L^{-1}. The aspect ratio (cell height to diameter, L/D) was fixed at 3 or 4. The dimensions of the scaled-up cells are listed in Table 2.

The temperature rise predicted for the center of the cell at $C/1$, $C/2$, $C/3$ and $C/6$ discharge rates, assuming a cooling rate of $h = 10$ W m^{-2} K^{-1} are shown in Fig. 6a and b for the 10 and 100 A h cells, respectively. The temperature rise at the end of discharge at $C/1$ rate is expected to be 42 and 60°C for the 10 and 100 A h cells, respectively. Simulation results demonstrate the insignificant effect of varying geometry (L/D), in the range of $L/D = 3$–4. This agrees with the low Biot number ($Bi = hL_c/k$) for a cooling rate of $h = 10$ W m^{-2} K^{-1}. The Biot number is less than 0.1 in the case of both scaled-up cells described here, so the cell may be considered a lumped system of uniform temperature. These results are in good agreement with results reported by Kanari et al. [24] however, at high discharge rates (e.g., at $C/1$ rate) and for all cooling conditions, our results showed higher temperature rise than their predictions for the 10 A h scaled-up cell.

Fig. 7a and b shows simulation results for both cells at $C/1$ discharge rate, assuming various cooling rates ($h = 1$, 5, 10, 20, 30, and 100 W m^{-2} K^{-1}). The temperature at the center is expected to rise about 80°C in the 100 A h cell at the end of discharge under near-insulating conditions ($h = 1$ W m^{-2} K^{-1}). If the initial temperature was above 30°C, this will cause the cell temperature to reach the lowest OTR point for the Sony cell. Under natural convection cooling conditions, e.g., $h = 5$ or 10 W m^{-2} K^{-1}, temperature rises of 70 and 60°C, respectively, are expected for the 100 A h cell. Temperature rises of 44 and 40°C are expected for the same cell under moderate forced convection, e.g., $h = 20$ and 30 W m^{-2} K^{-1}, respectively, while at high cooling rates ($h = 100$ W m^{-2} K^{-1}), the temperature rise should not exceed 25°C.

At low cooling rate, insignificant differences between simulated results are found for $L/D = 3$ and 4, while at high cooling rates, 2–5°C differences are noticed with Biot number values higher than (0.1). The value of the Biot number was found to be higher than 0.1 for both cells at high cooling rates, when $h = 100$ W m^{-2} K^{-1}. This will result in a temperature gradient inside the battery as shown in Fig. 8 for the 100 A h battery, where the cell center temperature is 7°C higher than the surface temperature. A temperature difference of 2–4°C results if h is in the range of 5–30 W m^{-2} K^{-1}. Almost no temperature gradient is noticed for near-insulating conditions ($h = 1$ W m^{-2} K^{-1}), where the Biot number is (Bi = 0.00544). This is in agreement with results reported by Kanari et al. [24] for similar cell design and operating conditions.

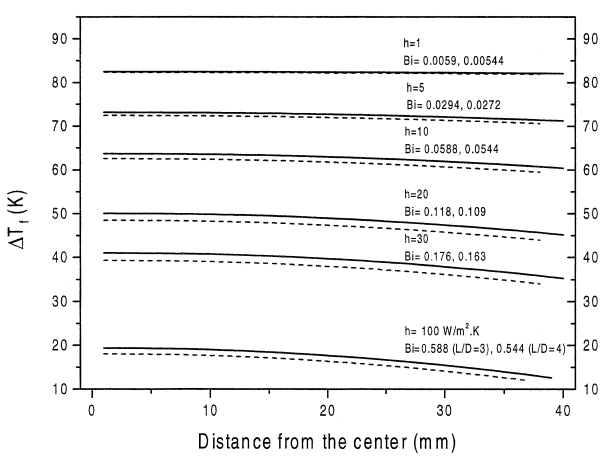

Fig. 8. Simulated temperature profile inside the 100 A h cell under different cooling conditions, discharge rate = $C/1$. ΔT_f: Temperature increase at the end of discharge.

7. Conclusions

A simplified one-dimensional thermal model with lumped parameters was developed to simulate temperature behaviour of Li-ion cell during discharge. The model was verified against temperature measurements at different discharge rates of the Sony US18650 cell.

Commercial Sony type lithium-ion cells at different open circuit potential were tested inside an ARC to determine their OTR temperatures. Experimental measurements showed that the thermal runaway reaction of slightly charged cells starts at significantly lower temperature than that of fully discharged cells. The results were used as temperature rise limits in the design of scaled-up Li-ion cells.

The simplified model was used to simulate temperature profiles of scaled-up lithium-ion cells of 10 and 100 A h capacity. The cell designs were based on the measured nominal capacity of the US18650 Sony cell and were assumed to contain the same materials and have the same chemistry. A cell aspect ratio (L/D) of 3 or 4 was used to fix the cell dimensions. Simulation results showed a significant effect of the cooling rate on the temperature rise of the cell for all discharge rates, this was not influenced by the L/D factor, in the range 3–4. The temperature non-uniformity of temperature inside the cell was found to be insignificant at low to moderate cooling rates, while a 7°C rise at the center was noticed at higher cooling rates, for $h = 100$ W m^{-2} K^{-1}. This is in agreement with the calculated Biot number under these conditions. Results showed that scaled-up cells of 10–100 A h are expected to

operate safely at low to moderate discharge rates under natural cooling conditions. At high discharge rates or under near-insulating conditions, cell temperature is expected to rise significantly, risking thermal runaway. Thermal management systems using active or passive cooling systems are required under such operating conditions.

8. Nomenclature

D	cell diameter (mm)
E	*cell voltage on load* (V)
E_{eq}	cell equilibrium voltage (V)
F	Faraday's constant
G	Gibbs free energy (J mol^{-1})
h	effective surface heat transfer coefficient (W m^{-2} K^{-1})
I	applied current (A)
k_{cell}	effective radial thermal conductivity of a cell (W m^{-1} K^{-1})
L	cell height (mm)
n	number of electrons
q	volumetric heat generation rate (W L^{-1})
Q	overall heat generation (J)
Q'	overall heat generation rate (W)
r	radial distance (mm)
R	cell radius (mm)
S	entropy (J mol^{-1} K^{-1})
t	time (s)
t_o	initial time (s)
T	cell temperature (K)
T_a	ambient temperature (K)
W_{el}	electric work (J)
α	thermal diffusivity (m^2 s^{-1})

Acknowledgements

This work was supported by the Army Research Office under Grant No. DAAH 04-94G-0055 and the Office of Naval Research under equipment Grant 5-57672, No. ARO DAAH 04-95-1-0569.

References

[1] J.S. Hong, H. Maleki, S. Al Hallaj, L. Redey, J.R. Selman, J. Electrochem. Soc. 145 (1998) 1489.
[2] Y. Saito, K. Kanari, K. Kanari, 8th Int. Mtg. Lithium Batteries, Nagoya, Japan, I-C-15, 1996.
[3] K. Kate, K. Takano, K. Nozaki, Y. Saito, A. Negishi, K. Kanari, 8th Int. Mtg. Lithium Batteries, Nagoya, Japan, I-C-14, 1996.
[4] Sony Type US18650 Lithium-Ion Battery Manual, Sony, 1993.
[5] A. Scot, G. Whitehead, Internal report (911916), Electrotek Concepts, 1991.
[6] J. Kim, T.V. Nguyen, R.E. White, J. Electrochem. Soc. 139 (1992) 10.
[7] Y. Chen, J.W. Evans, J. Electrochem. Soc. 140 (1993) 1833.
[8] M. Doyle, T.F. Fuller, J. Newman, J. Electrochem. Soc. 140 (1993) 1526.
[9] T.F. Fuller, M. Doyle, J. Newman, J. Electrochem. Soc. 141 (1994) 1.
[10] Y. Chen, J.W. Evans, J. Electrochem. Soc. 141 (1994) 2947.
[11] J. Newman, W. Tiedemann, J. Electrochem. Soc. 142 (1995) 1054.
[12] C.R. Pals, J. Newman, J. Electrochem. Soc. 142 (1995) 3274.
[13] C.R. Pals, J. Newman, J. Electrochem. Soc. 142 (1995) 3282.
[14] S. Al Hallaj, J.S. Hong, H. Maleki, J.R. Selman, EA 97-2, The Electrochemical Society, Pennington, NJ, 1997.
[15] Y. Chen, J.W. Evans, J. Electrochem. Soc. 143 (1996) 2708.
[16] L. Rao, J. Newman, J. Electrochem. Soc. 144 (1997) 2697.
[17] H. Maleki, S. Al Hallaj, J.R. Selman, Ralph B. Dinwiddie, H. Wang, Thermal properties of lithium-ion battery and components, J. Electrochem. Soc. 146 (1999) 947.
[18] CIS ARC Manual, Columbia Scientific Industries, Austin, TX, 1995.
[19] D.I. Townsend, J.C. Tou, J. Thermochim. Acta 37 (1980) 1.
[20] T. Maeda, N. Nakanishi, H. Kurokawa, K. Okita, T. Nohma, K. Nishio, Proceedings of the International Workshop on Lithium Batteries, Japan, 1B01, 1997, p. 181.
[21] K. Kanari, K. Takano, Y. Saito, T. Masuda, Proceedings of the International Workshop on Advanced Batteries, Japan, 3105, 1997, p. 83.
[22] M.S. Vreeke, D.T. Mah, M. Doyle, J. Electrochem. Soc. 145 (10) (1998) 3668.
[23] H.F. Gibard, J. Electrochem. Soc. 125 (1978) 353.
[24] K. Kanari, K. Takano, Y. Saito, Proceedings of International Workshop on Advanced Batteries, Japan, 1C07, in Japanese, 1998, p. 217.
[25] B.A. Johnson, R.E. White, J. Power Sources 70 (1998) 48–54.
[26] T. Miyamoto, H. Horie, The 39th Battery Symposium in Japan, 2I01, Nov. 1998.
[27] Y. Koga, M. Tohda, K. Katayama, Y. Nishi, The 39th Battery Symposium in Japan, 2I11, Nov. 1998.
[28] S. Oweis, G. Chagnon, T. Sack, A. Romero, L. d'Ussel, The 39th Battery Symposium in Japan, 2I07, Nov. 1998.
[29] T.I. Evans, R.E. White, J. Electrochem. Soc. 136 (1989) 2145.